HHS Public Access

Author manuscript

Gene. Author manuscript; available in PMC 2019 October 05.

Published in final edited form as:

Gene. 2018 October 05; 673: 95–101. doi:10.1016/j.gene.2018.06.048.

A Splice Junction-Targeted CRISPR Approach (spJCRISPR) Reveals Human *FOXO3B* To Be A Protein-Coding Gene

Evan E. Santo[1] and **Jihye Paik**[1,*]

[1]Department of Pathology and Laboratory Medicine, Weill Cornell Medical College, New York, NY 10065

Abstract

The rapid development of CRISPR technology is revolutionizing molecular approaches to the dissection of complex biological phenomena. Here we describe an alternative generally applicable implementation of the CRISPR-Cas9 system that allows for selective knockdown of extremely homologous genes. This strategy employs the lentiviral delivery of paired sgRNAs and nickase Cas9 (Cas9D10A) to achieve targeted deletion of splice junctions. This general strategy offers several advantages over standard single-guide exon-targeting CRISPR-Cas9 such as greatly reduced off-target effects, more restricted genomic editing, routine disruption of target gene mRNA expression and the ability to differentiate between closely related genes. Here we demonstrate the utility of this strategy by achieving selective knockdown of the highly homologous human genes *FOXO3A* and suspected pseudogene *FOXO3B*. We find the spJCRISPR strategy to efficiently and selectively disrupt FOXO3A and FOXO3B mRNA and protein expression; thus revealing that the human *FOXO3B* locus encodes a bona fide human gene. Unlike FOXO3A, we find the FOXO3B protein to be cytosolically localized in both the presence and absence of active Akt. The ability to selectively target and efficiently disrupt the expression of the closely-related *FOXO3A* and *FOXO3B* genes demonstrates the efficacy of the spJCRISPR approach.

Graphical Abstract

*Corresponding author: jep2025@med.cornell.edu, Phone: +1-212-746-6151, Fax: +1-212-746-6801.

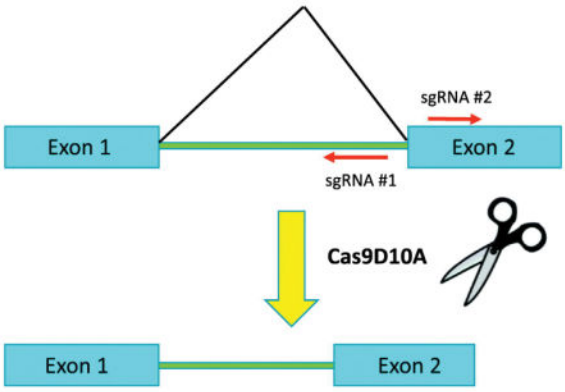

Keywords

FOXO3A; FOXO; Nickase; Cas9; Pseudogene

1. Introduction

CRISPR-Cas9 genome editing technology has been a major boon to modern molecular biology by providing a toolset for the efficient and rapid genetic engineering of cell lines and whole organisms (Hsu et al., 2014; Wright et al., 2016; Fellmann et al., 2017). In recent years much progress has been made in the refinement and deployment of CRISPR technology but some issues still remain. One particular challenge is the targeting of genes for deletion that have high sequence similarity to other genes. Another is the practicality of screening for successful disruption of gene expression where the gene product is poorly defined or antibodies are not of sufficient quality. Issues may also arise where disrupted genes produce alternative mRNAs and/or protein products that may obfuscate the interpretation of gene knockout results (Mou et al., 2017). Here we present a novel implementation of the CRISPR system that helps to address these practical problems by targeting mRNA splice junctions for deletion. We term this approach splice junction-targeting CRISPR (spJCRISPR). By disrupting gene splicing and hence mRNA maturation the expression of entire transcripts can be suppressed and/or rendered non-functional; which can be readily detected by RT-PCR. This is a marked improvement over standard CRISPR approaches which target exonic sequence with a single sgRNA and rely on the creation of frameshift mutations and premature stop codons to disable the gene product. Since intronic sequence is incorporated into the sgRNAs in addition to exonic sequence there are more possibilities for targeting closely related genes with much higher specificity than relying on single sgRNAs and limited sequence differences.

The forkhead box O (FOXO) subfamily of transcription factors consists of four members in mammals FOXO1 (FKHR), FOXO3A (FKHRL1), FOXO4 (AFX) and FOXO6 (Davis et al., 1995; Borkhardt et al., 1997; Anderson et al., 1998; Jacobs et al., 2003). Among the family members FOXO1 and FOXO3A are the most ubiquitously expressed while FOXO4 and FOXO6 exhibit more restricted expression patterns (Biggs et al., 2001; Chung et al., 2013). FOXOs are major effectors of cell signaling with their transcription factor activity being

strongly suppressed by the PI3K/Akt signaling pathway (Brunet et al., 1999; Kops et al., 1999). FOXOs have been implicated in many processes with some of the most important being apoptosis, cell cycle regulation, metabolism, longevity, response to oxidative stress, stem cell maintenance, cell-type specification, differentiation and immune response modulation (for review see Eijkelenboom and Burgering 2013).

Here we utilize our spJCRISPR approach to investigate the status of the human *FOXO3A* pseudogene, *FOXO3B*. Quite strikingly we find that the *FOXO3B* gene encodes a FOXO3A-related protein product and is therefore a true human gene. Unlike FOXO3A we find FOXO3B to have a much more limited expression pattern with its greatest enrichment in cerebellum, neural progenitor and embryonic stem cells. Although both FOXO3A and FOXO3B are phosphorylated by Akt FOXO3B remains constitutively cytosolic when Akt is inhibited whereas FOXO3A translocates to the nucleus.

2. Materials and Methods

2.1 Lentiviral Cloning

The CRISPRScan algorithm (Moreno-Mateos et al., 2015) was used to identify individual sgRNAs no more than 100 bp apart and in a “tail-to-tail” configuration (PAMs oriented away from each other) that could be used to target the selected FOXO3A and FOXO3B splice junctions. The control sgRNAs that comprise the no-target (NT) control construct were selected at random from the non-targeting control set of sgRNAs found within published sgRNA libraries (Doench et al., 2016). The sequence of all oligos used to clone the sgRNAs can be found in Supplemental Table 1. For each pair of sgRNAs one sgRNA was cloned into the pENTR L1-L4 U6 cassette and the other into the pENTR R4-R3 U6 cassette provided by the MuLE vector library after digestion of the vectors with BfuAI (Albers et al., 2015). The pENTR L3-L2 SV40 hCas9 vector from this library was modified to encode hCas9D10A by subcloning of the mutated fragment from pCAG hCas9D10A (Addgene # 52101) by digestion of both vectors with KpnI/BamHI. All pENTR clones were sequenced to ensure identity. The destination vector chosen for use in the multisite Clonase reaction was pLenti X1 Puro DEST (Addgene # 17297). LR Clonase II Plus (Thermo 12538) reactions were performed with 2 μl Clonase LR II Plus, 20 fmoles pLenti X1 Puro DEST, 10 fmoles of each sgRNA pENTR and 10 fmoles of pENTR hCas9D10A all to 10 μl volume in Tris-EDTA (TE) buffer pH 8. Reactions were allowed to proceed 20 hours at RT, followed by proteinase K treatment for 10 minutes at 37°C. Each reaction was transformed into 50 μl Stbl3 E. coli (Thermo C737303) and selected on 100 μg/ml ampicillin containing LB agar plates. To isolate clones Stbl3 colonies were grown at 25°C for 20 hours in LB medium containing 100 μg/ml ampicillin. Constructs were screened by sequencing and restriction digest to ensure no aberrant recombination. Ideal constructs were re-transformed into NEB Stable E. coli (NEB C3040H), grown at 37°C for 14 hours in LB containing 100 μg/ml ampicillin and midiprepped with the PureLink HiPure Plasmid Midiprep Kit (Thermo K210004) to eliminate endotoxins and provide high-quality DNA for virus production. It is of note that we found NEB Stable to be incompatible with Clonase reactions as they seem to be natively resistant to the CcdB suicide cassette in the destination vector which is essential for negative selection of non-recombinants. However, DNA prep quality (no smearing on

gel) and the stability of these lentiviral constructs propagated in NEB Stable was vastly superior to those propagated in Stbl3.

Gene synthesis (Biomatik) was used to synthesize the 290 amino acid FOXO3B ORF with the appended cloning sites HindIII (5′) and BamHI (3′). FOXO3B was excised on these sites and cloned into pENTR-MCS (Santo et al., 2013) digested with HindIII/BamHI. Wild-type human FOXO3A was cloned with the same strategy into pENTR-MCS. LR Clonase II (Thermo 11791100) reactions were performed with a modified form of the pInducer20 vector (Addgene #44012) where the Neo resistance cassette was replaced with a blasticidin resistance cassette. Recombination generated all-in-one lentiviral Dox-inducible overexpression constructs for FOXO3A and FOXO3B (both with no epitope tags). All clones were sequence confirmed.

2.2 Cell Culture & Virus Production

Puromycin and blasticidin were from Invivogen, DMSO, doxycycline and bovine insulin were from Sigma, MK-2206 was from Selleckchem. All plasticware was supplied by CELLSTAR. HEK293T cells were cultured in high glucose DMEM + pyruvate (Sigma D6429) containing 10% FBS and supplemented with HEPES to 20 mM, GlutaMAX to 1x, 10 U/ml penicillin and 10 μg/ml streptomycin. LHCNM2 myoblasts (Zhu et al., 2007) were grown on CELLSTAR plates coated with collagen from rat tail (Sigma C3867-1VL). Coating was done by incubating plates at 37°C for one hour with 10 μg/ml collagen dissolved in PBS. LHCNM2 growth medium was a 4:1 mixture of high glucose DMEM (Gibco 11965) and Medium 199 (Gibco 11150). Additional to this was 20 mM HEPES, 20% FBS, 0.03 μg/ml zinc sulfate (Sigma), 1.4 μg/ml vitamin B12 (Sigma), 0.055 μg/ml dexamethasone (Sigma), 2.5 ng/ml human HGF (Peprotech), 10 ng/ml human basic FGF (Peprotech), 10 U/ml penicillin and 10 μg/ml streptomycin. All cells were maintained in a water-jacketed incubator in a humidified atmosphere at 5% CO_2 and 37°C. All cell lines were tested for mycoplasma by PCR and found to be negative.

For viral packaging 1 14 cm dish of HEK293T cells at 80% confluency per construct was transfected with 4.5 μg pMD2.G, 9 μg psPAX2 and 18 μg of MuLE or pInducer construct using 80 μl of Fugene HD (Promega E2311). The day after transfection growth medium was discarded and replaced with 20 ml DMEM. 24 hours later this medium was collected and stored at 4°C and replaced with another 20 ml of DMEM. 24 hours later this 20 ml was collected and pooled with the previous 20 ml. All 40 ml was then filtered through a Stervix 0.45 um filter (Millipore, SVHVL10RC) with a 50 ml syringe and ultracentrifuged at 23,000 rpm for two hours at 4°C. The supernatant was removed and the viral pellet resuspended in 3 ml of Opti-MEM (Gibco 31985062) by vigorous pipetting followed by rocking at 4°C overnight to allow full dissolving. Virus was aliquoted and stored at −20°C. It is of note that PEI may also be used for the transfections but that viral titers obtained with Fugene HD were consistently at least 3x higher than those obtained with PEI.

For infection LHCNM2 cells were seeded at approximately 40% confluency in 6-well plates and infected with a gradient of virus for each construct typically ranging from 50 μl to 400 μl of the ultracentrifuged Opti-MEM resuspended virus. After 48 hours of incubation with the virus medium was changed and cells were selected with 8 μg/ml puromycin for an

additional 48 hours (MuLE construct) or 10 μg/ml blasticidin (pInducer FOXO3A and FOXO3B constructs). Cells were then passed to 6 cm plates and maintained on appropriate selection agents for an additional 48 hours.

2.3 Genomic & RT-PCR

Genomic DNA was isolated with the GeneJET Genomic DNA Purification Kit (Thermo K0721) following the standard protocol. Total RNA was harvested with Trizol (Thermo 15596026) following the standard protocol. Both were quantitated by Nanodrop 260/280 absorbance reading. cDNA was synthesized with the RevertAid First Strand cDNA Synthesis Kit (Thermo K1622) using the Random Hexamer primer and 1 μg of total RNA following the standard protocol. cDNA was diluted 1:5 in dH2O and 1 μl of cDNA was used per RT-PCR reaction. RT-qPCR was performed with PowerUp SYBR Green Master Mix (Thermo A25741) on a 7500 Fast Real Time PCR System (Applied Biosystems) using 15 μl reaction volumes in a 96-well plate format. Due to the very high GC content of FOXO3B the PCR additives DMSO and Betaine were used to enhance the specificity and efficiency of FOXO3B PCR reactions. All primers and PCR conditions can be found in Supplemental Table 2. Ethidium bromide stained agarose gel bands were quantified using the ImageJ package.

2.4 Western Blotting

Protein lysates were harvested in 1x Laemmli lysis buffer containing protease and phosphatase inhibitors and quantitated with the DC Protein Assay kit (Biorad 5000116). Lysates were then diluted to appropriate concentrations in 6x sample buffer, boiled for 10 minutes and resolved on 8% SDS-PAGE gels. Gels were wet transferred (20% methanol) to Amersham Protran Premium 0.45 um NC membrane (GE Healthcare 10600003) at 100 volts and 4°C for two hours. After Ponceau S staining membranes were blocked in 5% Milk TBS at RT for one hour then incubated with primary antibodies at appropriate dilutions in 3% BSA TBS + 0.1% Tween 20 (TBST) overnight rocking at 4°C. Membranes were then washed three times with TBST and incubated with appropriate HRP-conjugated secondary antibody diluted in 5% Milk TBST for one hour at RT. ECL and film was used for signal detection. The FOXO3A (#2497), pThr24/32 FOXO1/3 (#9464) and pSer473 Akt (#4060) antibodies were all from Cell Signaling and used at 1:1000 dilutions.

2.5 Immunofluorescence

LHCNM2 myoblasts were seeded in 24-well plates. After treatments they were fixed with 4% PFA for 15 minutes, permeabilized with 0.2% Triton X-100 for 5 minutes, washed 3x with PBS then incubated with a 1:1000 dilution of FOXO3A antibody (Cell Signaling #2497) in 3% BSA TBST overnight at 4°C rocking. The next day primary antibody was removed and cells were stained with PBS containing 1:1000 Alexa Fluor 488 Rabbit secondary (Thermo A21206) and 1:50000 DAPI at RT for one hour. After washing with PBS cells were imaged on an EVOS FL Auto Cell Imaging System (Thermo).

3. Results

3.1 The human FOXO3B locus encodes a novel splice product

While attempting to design specific sgRNAs against the coding exons of human *FOXO3A* for use in a standard CRISPR approach it was noticed that the putative sgRNAs were also mapping to the human *FOXO3B* locus with 100% specificity. Across the replicated coding sequence of *FOXO3A* at the *FOXO3B* locus there is 99% sequence identity which proved to be a major complication in FOXO3A polymorphism studies (Flachsbart et al., 2013). *FOXO3B* is an intron-less reverse transcribed copy of the canonical FOXO3A transcript reinserted into a duplication of the *ZNF286A* locus; *ZNF286B* on chromosome band 17p11.2 (Fig. 1A). Sequence alignment of the full FOXO3A and ZNF286A transcripts to this locus reveals that this reinsertion places the 5′ end of FOXO3A downstream of three ZNF286B putative coding exons all in reverse strand orientation (Fig. 1A). It has been demonstrated that the *FOXO3B* locus (previously termed FKHRL1P1) does encode an mRNA that is expressed at low levels throughout human tissues (Anderson et al., 1998). Being that the ZNF286A-derived exons and the 5′ end of the FOXO3A reinsertion are only separated by 7559 bp we performed RT-PCR with forward primers designed within the ZNF286A-derived exons and reverse primers within the FOXO3A reinsertion and successfully detected a spliced fusion product expressed in HEK293T cDNA (data not shown) which we termed FOXO3B (aligned transcript Figure 1A; deposited in Genbank under accession number MG753997). Interestingly, the *FOXO3B* locus and transcript may be entirely unique to humans as the FOXO3A reinsertion is not seen in the genomic alignments of the *FOXO3B* locus to chimpanzee or other primate and non-primate species (Fig. 1A).

Analysis of the FOXO3B splice product identified an ATG (252 bp) located in the second ZNF286A-derived exon that falls in-frame with the FOXO3A-derived coding sequence with a stop codon at 1124 bp. This yields a predicted protein product of 290 amino acids that is essentially a fusion between the n-terminal residues of ZNF286A and the n-terminal residues of FOXO3A (Fig. 1B). Analysis of this sequence yields no clear protein domains aside from a portion of the forkhead domain encoded by the FOXO3A sequence. This protein sequence does not include DNA contact residues (Tsai et al., 2007). However, an Akt phosphorylation site of FOXO3A (Thr32 equivalent, Thr117) is retained (Brunet et al., 1999). RT-qPCR for this gene product was performed across a panel of human tissues and cell lines using primers spanning the ZNF286A/FOXO3A splice junction ensuring their uniqueness. With the exception of adult cerebellum and whole fetal brain FOXO3B is generally of low expression in all tissues tested (Fig. 1C). FOXO3B seems to be much more highly expressed in cell lines generally and in neural progenitor cells (SY5Y and H9-derived NPCs) in particular than in differentiated tissues (Fig. 1C).

3.2 The spJCRISPR approach efficiently and specifically deletes FOXO3A and FOXO3B

With knowledge of the structure of the FOXO3B transcript we decided to develop a CRISPR strategy to target both *FOXO3A* and *FOXO3B* independently for deletion while also avoiding any perturbation of *ZNF286A*. To this end we thought it most efficient and specific to incorporate both intronic and exonic sequence into the targeting strategy; targeting splice

junctions unique to each transcript for deletion. To enforce this specificity we chose to use a nickase form of Cas9 (Cas9D10A) in conjunction with two sgRNAs per genomic target site (Ran et al., 2013). It has been found empirically that these paired sgRNAs should be arranged in a “tail-to-tail” orientation with the PAM targeting each strand oriented in opposite directions from each other (Shen et al., 2014). We found optimal targeting pairs against the donor splice site of FOXO3A exon #2 and the acceptor splice site of FOXO3B exon #4 (Fig. 2A).

To facilitate the efficient delivery of the sgRNAs and Cas9D10A to the target cells we chose to construct an all-in-one lentiviral vector using the MuLE lentiviral cloning system (Albers et al., 2015). This enabled the building of a single vector for each pair of sgRNAs containing two separate U6 sgRNA cassettes, an SV40-driven hCas9D10A and a PGK-driven puromycin resistance gene using a single multisite Clonase reaction (Fig. 2B). In addition to the constructs targeting *FOXO3A* and *FOXO3B* a control construct was generated containing a pair of two non-targeting sgRNAs (NT).

We infected LHCNM2 human myoblasts with the NT, FOXO3A and FOXO3B construct viruses and selected the cells on puromycin for four days. Following this the lines were cultured for an additional week at which point they were harvested for genomic DNA, total RNA and protein. Genomic PCR using primers flanking the target regions of the FOXO3A and FOXO3B constructs (Fig. 2A) showed successfully disruption of these target sites with their respective constructs (Fig. 3A). To test the effect of these deletions on transcript expression FOXO3A mRNA levels were measured by RT-qPCR using unique primers designed within the 3pUTR (Fig. 2A). The FOXO3A construct gave a 65% decrease in FOXO3A mRNA levels (Fig. 3B, Student’s T-test two-sided $p < 0.0001$) while the FOXO3B construct yielded an insignificant 12% decrease in FOXO3A mRNA levels (Fig. 3B, Student’s T-test two-sided $p > 0.05$). FOXO3B mRNA levels were also evaluated by RT-PCR across these constructs (Fig. 3C). With the FOXO3A construct there is a slight decrease in FOXO3B mRNA levels whereas FOXO3B mRNA is nearly abolished by the FOXO3B construct (Fig. 3C). Taken together these results demonstrate that the FOXO3A and FOXO3B spJCRISPR constructs achieved massive disruption of their respective genomic and mRNA targets with a high degree of specificity.

3.3 The FOXO3B mRNA encodes a 220 amino acid protein with a constitutively cytosolic localization pattern

Next we decided to assess FOXO3A and FOXO3B expression on the protein level. As FOXO3B has never before been observed on western blot we cloned the exact 290 amino acid FOXO3B ORF into a Dox-inducible lentiviral expression vector and derived a stable LHCNM2 FOXO3B inducible overexpression line. Western blotting of protein lysates from this line using an n-terminal FOXO3A antibody revealed an exogenous protein product of 44 KDa (Fig. 3D). We next probed a western blot loaded with the lysates harvested from the LHCNM2 lines infected with the NT, FOXO3A and FOXO3B constructs with the same antibody and observed two primary bands; FOXO3A at 90 KDa and putative FOXO3B at 44 KDa (Fig. 3E). The FOXO3A construct abolished FOXO3A protein expression and had no effect on the FOXO3B band while the FOXO3B construct strongly reduced FOXO3B

expression while leaving FOXO3A expression unchanged (Fig. 3E). These experiments again demonstrate the efficacy and specificity of the spJCRISPR constructs as well as identify endogenous FOXO3B protein for the first time.

Being that FOXO3A subcellular localization is tightly controlled by Akt-mediated phosphorylation (Brunet et al., 1999) we assessed both the phosphorylation of FOXO3B at the putative Akt site Thr117 as well as its localization by immunofluorescence. Stimulation of FOXO3B overexpressing cells with insulin demonstrated high levels of phosphorylated Thr117 which was completely ablated by treatment with the Akt inhibitor (referred to as Akti) MK-2206 (Fig. 4A). Unlike FOXO3A, FOXO3B was found to be exclusively localized to the cytosol under both conditions (Fig. 4B and Fig. 4C). From these findings we concluded that Akt phosphorylates FOXO3B at Thr117 but that this event does not determine the subcellular localization of the FOXO3B protein.

4. Discussion

Here we describe a new CRISPR approach (spJCRISPR) that may have wide general utility. We have used this method to genetically dissect the closely-related human *FOXO3A* and *FOXO3B* loci; in the process redefining human *FOXO3B* as a bona fide human gene. spJCRISPR offers a number of advantages over standard single-guide CRISPR approaches. Many of these advantages stem from the reliance on single-strand nickase Cas9 (Cas9D10A) used in conjunction with sgRNA pairs that incorporate intronic sequence. One major advantage is the vastly reduced expected number of off-target effects when using Cas9D10A (Ran et al., 2013; Chiang et al., 2016). This is much more appropriate than standard CRISPR to the construction of stable cell lines by lentiviral delivery where both the delivered Cas9 and sgRNAs will be persistently expressed; increasing the probability of accumulating off-target genomic disruptions in time. It could also be argued that a much more restricted genomic disruption that maximizes interference with gene expression is preferable to potentially larger unrestricted deletions/insertions caused by single sgRNA approaches used with wild-type Cas9. As the DNA repair step is restricted to the region between the two single-strand nicks using sgRNAs that may be maximally 100 bp apart the target region is much more limited whereas with a single dsDNA break much larger insults are possible. The more restricted editing of a nickase approach greatly reduces the unwanted effects of disrupting surrounding gene regulatory elements and may readily allow the deletion of specific gene isoforms in a controlled way. Furthermore, specific targeting of splice junctions offers a much higher probability of consistent disruption of not just coding sequence and hence protein production but also formation of the entire mature mRNA. This reduction of viable mature mRNA may guard against the production of unnatural protein products that could result from a standard CRISPR approach. Since the targeting of the gene is limited to a single splice junction PCR strategies can also be rationally designed to assess exon skipping resulting in unnatural transcripts. Exon skipping is an increasingly appreciated artifact of CRISPR approaches to gene knockout (Mou et al., 2017). To combat this problem pairs of sgRNAs and target splice junctions could then be selected within a gene to achieve optimal knockout results. Screening for knockout is also made somewhat more direct by spJCRISPR due to the expectation that mRNA expression will be routinely disrupted; enabling the use of RT-PCR across the targeted splice junction as was done with

FOXO3B or even primers 3′ of the target site as was the case with FOXO3A (Fig. 2A, Fig. 3B and Fig. 3C). This is especially useful in cases where there are poor antibodies for a gene product and/or the gene product is undefined. Incorporating intronic sequence into the targeting strategy also allows for straightforward gene rescue experiments to be performed. An unmodified transgene could be stably introduced into cells stably expressing the Cas9D10A and sgRNAs without having the complication of it being deleted and/or suppressed by the Cas9/sgRNA complexes.

As demonstrated here another major advantage of the spJCRISPR approach is in achieving specificity among closely related genes and/or putative pseudogenes with uninvestigated functions. As the human genome is estimated to contain up to 14,000 pseudogenes (Milligan and Lipovich 2014) and 842 gene families (Gray et al., 2016) this is a non-trivial issue. Here we present a microcosm of this conundrum by reinterrogating the status of the human *FOXO3B* pseudogene. We cloned additional 5′ exons derived from the duplication of *ZNF286A* beyond which were known to exist when *FOXO3B* was first identified (Anderson et al., 1998); therefore identifying a longer splice product and a 220 amino acid ORF. Using the spJCRISPR strategy we were able to target *FOXO3A* and *FOXO3B* independently confirming genomic, transcript and protein deletions by each construct for their respective targets. The strong knockdown of FOXO3A on the protein level precludes that the FOXO3 western blot band at 44 KDa is a processed form of the full length FOXO3A protein (Fig. 3E). This band is still present at control levels with the FOXO3A knockdown (Fig. 3E). This observation further strengthens the argument that this band is indeed endogenous FOXO3B as the FOXO3B knockdown and detection with this particular n-terminal antibody suggests. This successfully identifies FOXO3B as a true human gene rather than a pseudogene.

Many studies in human cell lines have relied on siRNAs and shRNAs to interrogate endogenous functions of FOXO3A (Ido et al., 2015; Lu et al., 2015; Brucker et al., 2016; Kumazoe et al., 2017; Rupp et al., 2017). Given the extreme similarity between the FOXO3A and FOXO3B mRNA sequences and the seemingly general expression of FOXO3B in human cell lines it is highly likely that FOXO3B mRNA and protein expression was impaired along with that of FOXO3A in many of these studies; potentially complicating the interpretation of previous results. Recently, it has been reported that targeting the FOXO3B mRNA (referred to as “Foxo3P”) with siRNAs of unspecified sequence resulted in the reduction of FOXO3A protein levels but not FOXO3A mRNA levels (Yang et al., 2016). The claimed mechanism was that reduction of FOXO3B mRNA levels resulted in the increased activity of FOXO3A-suppressing miRNAs since they were not being “sponged” by the FOXO3B mRNA. Our highly specific knockdown of the FOXO3B mRNA argues against this being a general mechanism as we observed no reduction in FOXO3A protein levels (Fig. 3E). As FOXO3B can no longer simply be regarded as a pseudogene it is also possible that some of the functional data in the Yang et al. study may need to be reinterpreted. For instance, the rescue of cell viability from hydrogen peroxide treatment conferred by the FOXO3B siRNAs may have been due to FOXO3B protein reduction rather than a decrease in FOXO3A protein levels. More careful studies will be necessary to segregate FOXO3A and FOXO3B mRNA and protein functions in the future. These studies will be greatly enabled by these FOXO3A and FOXO3B-specific spJCRISPR constructs.

Further investigation into the biological role of *FOXO3B* is now warranted. It is particularly interesting that *FOXO3B* may be entirely specific to humans as the chimpanzee and other primate genomes do not contain a complete version of this locus. Many human-specific genes are thought to play an outsized role in brain development (Konopka et al., 2012; Bae et al., 2015). In this regard the limited expression of FOXO3B across most tissues with the highest expression levels being achieved in neural progenitor cells and whole fetal brain with very low expression in whole adult brain (yet with high expression in adult cerebellum; Fig. 1C) may point to a role for FOXO3B in neural progenitor maintenance and/or neuronal development. Indeed, this is a well-established compartment for critical FOXO functions (Paik et al., 2009; Renault et al., 2009; Yeo et al., 2013; Hwang et al., 2017). Mechanistically, FOXO3B may challenge our normal perception of the FOXO family as purely playing the role of transcription factors. Since FOXO3B is constitutively cytosolic and lacking critical regions of the forkhead domain involved in DNA binding along with nuclear import and export signals it is unlikely to have nuclear functions. Additional genetic and biochemical studies will be required to uncover its alternative roles.

Supplementary Material

Refer to Web version on PubMed Central for supplementary material.

Acknowledgments

Funding

This work was supported by the National Institutes of Health [grant number AG048284].

Abbreviations

aa	amino acid(s)
bp	base pairs
Cas9	CRISPR associated protein 9
cDNA	DNA complementary to RNA
CRISPR	Clustered Regularly Interspaced Short Palindromic Repeats
DMSO	dimethylsulfoxide
Dox	doxycycline
dsDNA	double stranded DNA
FOXO	forkhead box O
MCS	multiple cloning site
MOI	multiplicity of infection
mRNA	messenger RNA

NES	nuclear export signal
NLS	nuclear localization signal
nt	nucleotide(s)
ORF	open reading frame
PAM	protospacer adjacent motif
PI3K	phosphoinositide 3-kinase
RT-PCR	reverse transcriptase polymerase chain reaction
SD	standard deviation
SDS-PAGE	sodium dodecyl sulfate polyacrylamide gel electrophoresis
sgRNA	short guide RNA
UTR	untranslated region
ZNF286	zinc finger protein 286

References

Albers J, Danzer C, Rechsteiner M, Lehmann H, Brandt LP, Hejhal T, Catalano A, Busenhart P, Goncalves AF, Brandt S, et al. A versatile modular vector system for rapid combinatorial mammalian genetics. J Clin Invest. 2015; 125:1603–1619. [PubMed: 25751063]

Anderson MJ, Viars CS, Czekay S, Cavenee WK, Arden KC. Cloning and characterization of three human forkhead genes that comprise an FKHR-like gene subfamily. Genomics. 1998; 47:187–199. [PubMed: 9479491]

Bae BI, Jayaraman D, Walsh CA. Genetic changes shaping the human brain. Dev Cell. 2015; 32:423–434. [PubMed: 25710529]

Biggs WH III, Cavenee WK, Arden KC. Identification and characterization of members of the FKHR (FOX O) subclass of winged-helix transcription factors in the mouse. Mamm Genome. 2001; 12:416–425. [PubMed: 11353388]

Borkhardt A, Repp R, Haas OA, Leis T, Harbott J, Kreuder J, Hammermann J, Henn T, Lampert F. Cloning and characterization of AFX, the gene that fuses to MLL in acute leukemias with a t(X;11)(q13;q23). Oncogene. 1997; 14:195–202. [PubMed: 9010221]

Brucker DP, Maurer GD, Harter PN, Rieger J, Steinbach JP. FOXO3a orchestrates glioma cell responses to starvation conditions and promotes hypoxia-induced cell death. Int J Oncol. 2016; 49:2399–2410. [PubMed: 27840901]

Brunet A, Bonni A, Zigmond MJ, Lin MZ, Juo P, Hu LS, Anderson MJ, Arden KC, Blenis J, Greenberg ME. Akt promotes cell survival by phosphorylating and inhibiting a Forkhead transcription factor. Cell. 1999; 96:857–868. [PubMed: 10102273]

Chiang TW, le SC, Larrieu D, Demir M, Jackson SP. CRISPR-Cas9(D10A) nickase-based genotypic and phenotypic screening to enhance genome editing. Sci Rep. 2016; 6:24356. [PubMed: 27079678]

Chung SY, Huang WC, Su CW, Lee KW, Chi HC, Lin CT, Chen ST, Huang KM, Tsai MS, Yu HP, et al. FoxO6 and PGC-1alpha form a regulatory loop in myogenic cells. Biosci Rep. 2013:33.

Davis RJ, Bennicelli JL, Macina RA, Nycum LM, Biegel JA, Barr FG. Structural characterization of the FKHR gene and its rearrangement in alveolar rhabdomyosarcoma. Hum Mol Genet. 1995; 4:2355–2362. [PubMed: 8634710]

Doench JG, Fusi N, Sullender M, Hegde M, Vaimberg EW, Donovan KF, Smith I, Tothova Z, Wilen C, Orchard R, et al. Optimized sgRNA design to maximize activity and minimize off-target effects of CRISPR-Cas9. Nat Biotechnol. 2016; 34:184–191. [PubMed: 26780180]

Eijkelenboom A, Burgering BM. FOXOs: signalling integrators for homeostasis maintenance. Nat Rev Mol Cell Biol. 2013; 14:83–97. [PubMed: 23325358]

Fellmann C, Gowen BG, Lin PC, Doudna JA, Corn JE. Cornerstones of CRISPR-Cas in drug discovery and therapy. Nat Rev Drug Discov. 2017; 16:89–100. [PubMed: 28008168]

Flachsbart F, Moller M, Daumer C, Gentschew L, Kleindorp R, Krawczak M, Caliebe A, Schreiber S, Nebel A. Genetic investigation of FOXO3A requires special attention due to sequence homology with FOXO3B. Eur J Hum Genet. 2013; 21:240–242. [PubMed: 22588664]

Gray KA, Seal RL, Tweedie S, Wright MW, Bruford EA. A review of the new HGNC gene family resource. Hum Genomics. 2016; 10:6. [PubMed: 26842383]

Hsu PD, Lander ES, Zhang F. Development and applications of CRISPR-Cas9 for genome engineering. Cell. 2014; 157:1262–1278. [PubMed: 24906146]

Ido Y, Duranton A, Lan F, Weikel KA, Breton L, Ruderman NB. Resveratrol prevents oxidative stress-induced senescence and proliferative dysfunction by activating the AMPK-FOXO3 cascade in cultured primary human keratinocytes. PLoS One. 2015; 10:e0115341. [PubMed: 25647160]

Jacobs FM, van der Heide LP, Wijchers PJ, Burbach JP, Hoekman MF, Smidt MP. FoxO6, a novel member of the FoxO class of transcription factors with distinct shuttling dynamics. J Biol Chem. 2003; 278:35959–35967. [PubMed: 12857750]

Konopka G, Friedrich T, Davis-Turak J, Winden K, Oldham MC, Gao F, Chen L, Wang GZ, Luo R, Preuss TM, et al. Human-specific transcriptional networks in the brain. Neuron. 2012; 75:601–617. [PubMed: 22920253]

Kops GJ, de Ruiter ND, De Vries-Smits AM, Powell DR, Bos JL, Burgering BM. Direct control of the Forkhead transcription factor AFX by protein kinase B. Nature. 1999; 398:630–634. [PubMed: 10217147]

Kumazoe M, Takai M, Bae J, Hiroi S, Huang Y, Takamatsu K, Won Y, Yamashita M, Hidaka S, Yamashita S, et al. FOXO3 is essential for CD44 expression in pancreatic cancer cells. Oncogene. 2017; 36:2643–2654. [PubMed: 27893718]

Lu H, Samanta D, Xiang L, Zhang H, Hu H, Chen I, Bullen JW, Semenza GL. Chemotherapy triggers HIF-1-dependent glutathione synthesis and copper chelation that induces the breast cancer stem cell phenotype. Proc Natl Acad Sci USA. 2015; 112:E4600–E4609. [PubMed: 26229077]

Milligan MJ, Lipovich L. Pseudogene-derived lncRNAs: emerging regulators of gene expression. Front Genet. 2014; 5:476. [PubMed: 25699073]

Moreno-Mateos MA, Vejnar CE, Beaudoin JD, Fernandez JP, Mis EK, Khokha MK, Giraldez AJ. CRISPRscan: designing highly efficient sgRNAs for CRISPR-Cas9 targeting in vivo. Nat Methods. 2015; 12:982–988. [PubMed: 26322839]

Mou H, Smith JL, Peng L, Yin H, Moore J, Zhang XO, Song CQ, Sheel A, Wu Q, Ozata DM, et al. CRISPR/Cas9-mediated genome editing induces exon skipping by alternative splicing or exon deletion. Genome Biol. 2017; 18:108. [PubMed: 28615073]

Paik JH, Ding Z, Narurkar R, Ramkissoon S, Muller F, Kamoun WS, Chae SS, Zheng H, Ying H, Mahoney J, et al. FoxOs cooperatively regulate diverse pathways governing neural stem cell homeostasis. Cell Stem Cell. 2009; 5:540–553. [PubMed: 19896444]

Ran FA, Hsu PD, Lin CY, Gootenberg JS, Konermann S, Trevino AE, Scott DA, Inoue A, Matoba S, Zhang Y, et al. Double nicking by RNA-guided CRISPR Cas9 for enhanced genome editing specificity. Cell. 2013; 154:1380–1389. [PubMed: 23992846]

Renault VM, Rafalski VA, Morgan AA, Salih DA, Brett JO, Webb AE, Villeda SA, Thekkat PU, Guillerey C, Denko NC, et al. FoxO3 regulates neural stem cell homeostasis. Cell Stem Cell. 2009; 5:527–539. [PubMed: 19896443]

Rupp M, Hagenbuchner J, Rass B, Fiegl H, Kiechl-Kohlendorfer U, Obexer P, Ausserlechner MJ. FOXO3-mediated chemo-protection in high-stage neuroblastoma depends on wild-type TP53 and SESN3. Oncogene. 2017; 36:6190–6203. [PubMed: 28869600]

Santo EE, Stroeken P, Sluis PV, Koster J, Versteeg R, Westerhout EM. FOXO3a is a major target of inactivation by PI3K/AKT signaling in aggressive neuroblastoma. Cancer Res. 2013; 73:2189–2198. [PubMed: 23378341]

Shen B, Zhang W, Zhang J, Zhou J, Wang J, Chen L, Wang L, Hodgkins A, Iyer V, Huang X, et al. Efficient genome modification by CRISPR-Cas9 nickase with minimal off-target effects. Nat Methods. 2014; 11:399–402. [PubMed: 24584192]

Tsai KL, Sun YJ, Huang CY, Yang JY, Hung MC, Hsiao CD. Crystal structure of the human FOXO3a-DBD/DNA complex suggests the effects of post-translational modification. Nucleic Acids Res. 2007; 35:6984–6994. [PubMed: 17940099]

Wright AV, Nunez JK, Doudna JA. Biology and Applications of CRISPR Systems: Harnessing Nature's Toolbox for Genome Engineering. Cell. 2016; 164:29–44. [PubMed: 26771484]

Yang W, Du WW, Li X, Yee AJ, Yang BB. Foxo3 activity promoted by non-coding effects of circular RNA and Foxo3 pseudogene in the inhibition of tumor growth and angiogenesis. Oncogene. 2016; 35:3919–3931. [PubMed: 26657152]

Yeo H, Lyssiotis CA, Zhang Y, Ying H, Asara JM, Cantley LC, Paik JH. FoxO3 coordinates metabolic pathways to maintain redox balance in neural stem cells. EMBO J. 2013; 32:2589–2602. [PubMed: 24013118]

Zhu CH, Mouly V, Cooper RN, Mamchaoui K, Bigot A, Shay JW, Di Santo JP, Butler-Browne GS, Wright WE. Cellular senescence in human myoblasts is overcome by human telomerase reverse transcriptase and cyclin-dependent kinase 4: consequences in aging muscle and therapeutic strategies for muscular dystrophies. Aging Cell. 2007; 6:515–523. [PubMed: 17559502]

Highlights

- Standard CRISPR approaches have limitations targeting closely related genes.
- spjCRISPR is a novel implementation of CRISPR-Cas9 targeting gene splice junctions.
- spJCRISPR enables efficient and specific knockdown of highly similar genes.
- The human FOXO3B gene is a protein-coding gene and not a pseudogene.
- spJCRISPR offers numerous advantages over standard CRISPR approaches.

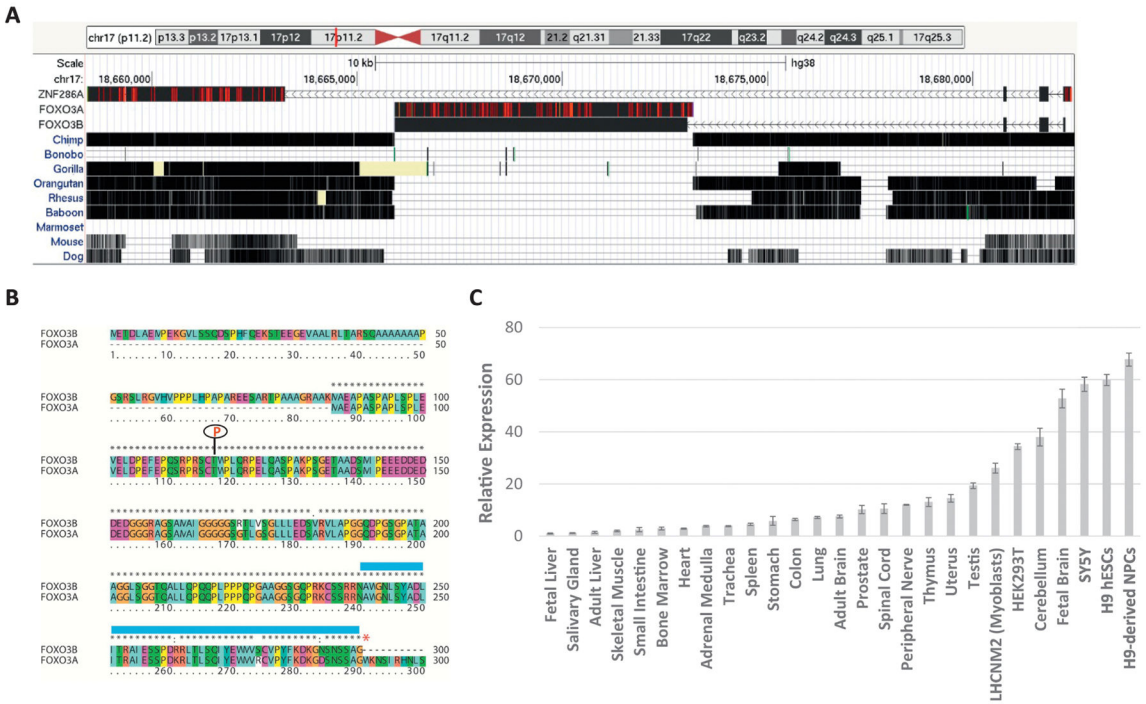

Fig. 1.

The human genome encodes a FOXO3A-related transcript, FOXO3B. A. BLAT alignment of the ZNF286A, FOXO3A and FOXO3B transcripts to the *FOXO3B* (aka *ZNF286B*) locus on 17p11.2 (Hg38 assembly) with the mammalian conservation track shown (UCSC Genome Browser). Red hash marks within the aligned sequence indicate sequence mismatches between the aligned transcript sequence and the genome. B. Protein sequence alignment of FOXO3A and predicted FOXO3B protein. The blue bar above the sequence indicates the forkhead domain, the red asterisk the FOXO3B stop codon and the red 'P' the FOXO3A Akt phosphorylation site (Thr32 FOXO3A, Thr117 FOXO3B). C. RT-qPCR measurement of FOXO3B expression across a panel of human cell lines and tissues normalized to 18S rRNA and calculated relative to the expression in fetal liver using the ΔΔCt method. Errors bars are SD of three replicates.

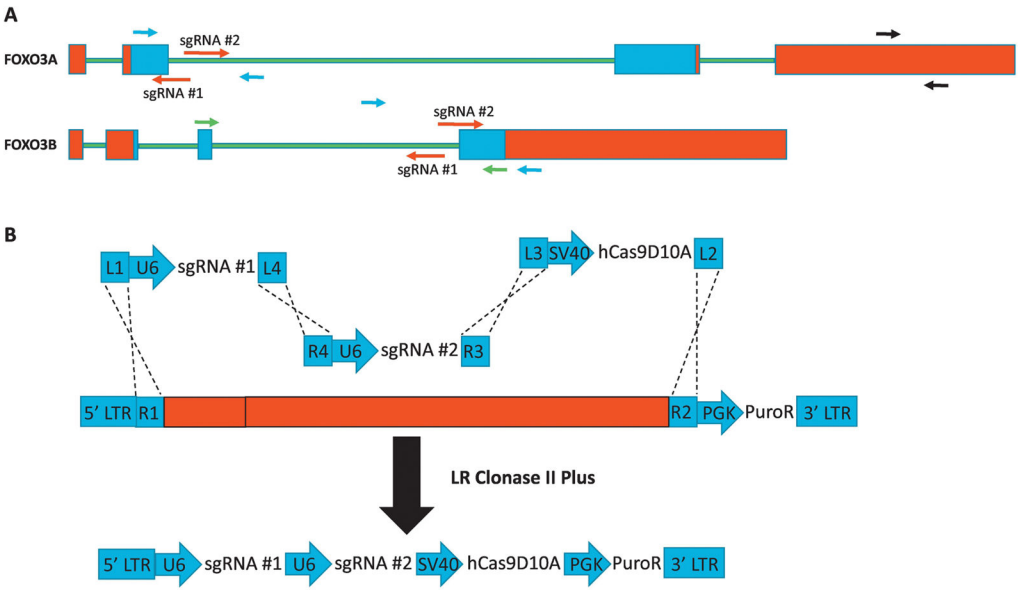

Fig. 2.

FOXO3A and *FOXO3B* can be targeted for deletion independently with the spJCRISPR approach. A. Cartoon depiction of spJCRISPR targeting strategy for *FOXO3A* and *FOXO3B* loci. Red indicates 5p and 3p UTRs, green intronic sequence and blue protein coding sequence. Red arrows indicate sgRNAs, black arrows primers used for both RT-PCR and genomic PCR, blue arrows primers used for genomic PCR only and green arrows RT-PCR only. B. A cartoon depiction of the multisite Clonase strategy utilizing modified MuLE entry vectors.

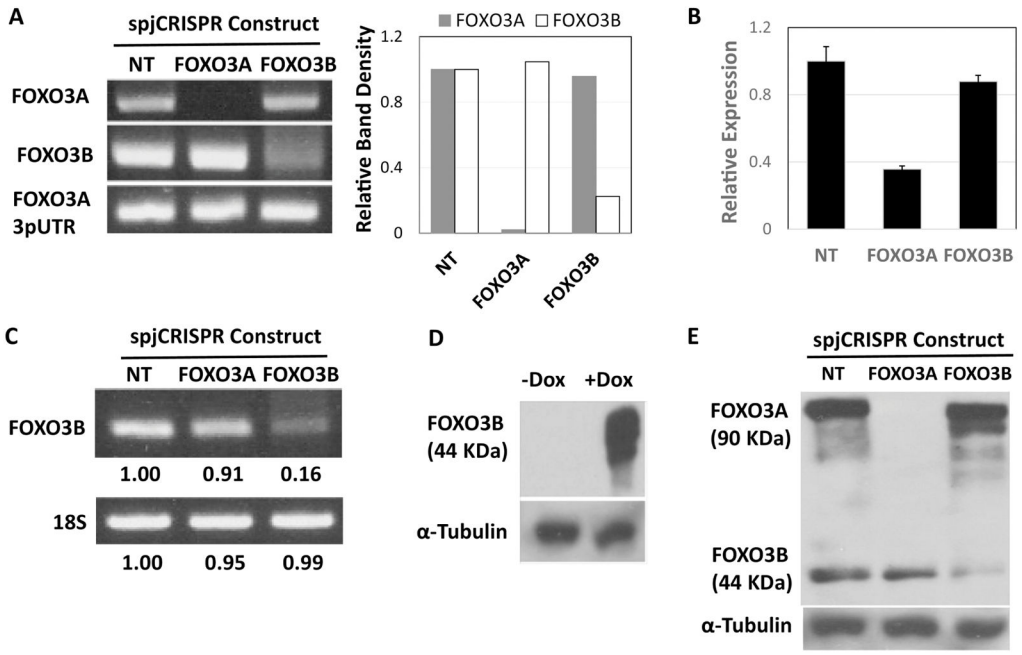

Fig. 3.

spJCRISPR achieves specific knockdown of FOXO3A and FOXO3B on the mRNA and protein level. A. Genomic PCR using primers flanking the *FOXO3A* and *FOXO3B* target sites for the respective spJCRISPR constructs. LHCNM2 myoblasts were infected with the described constructs and selected on puromycin. A week following selection genomic DNA was harvested and PCR performed (35 cycles). Primers specific to sequence in the *FOXO3A* 3pUTR were used as a loading control. Band densitometry was done by normalizing all bands to their respective NT construct band intensities. Primer pair locations are annotated in Figure 2A. B. RT-qPCR of FOXO3A mRNA using the FOXO3A-specific 3pUTR primers from RNA harvested in parallel with the gDNA. FOXO3A mRNA measurements were normalized to 18S rRNA and calculated relative to cells infected with the NT construct using the ΔΔCt method. Errors bars are SD of four replicates. Primer locations are annotated in Figure 2A. C. RT-PCR of FOXO3B mRNA using FOXO3B-specific primers and 18S rRNA primers as a loading control from the RNA harvested in parallel with the gDNA (35 cycles). Band densitometry was done as in Figure 3A. Primer locations are annotated in Figure 2A. D. Overexpression of FOXO3B in LHCNM2 myoblasts infected with a Dox-inducible FOXO3B expression construct. +Dox cells were treated with 0.1 ug/ml Dox for 48 hours and protein harvested. The western blot was performed with a monoclonal FOXO3A antibody raised against FOXO3A n-terminal residues with the epitope centered on Glu50 (Cell Signaling #2497). α-Tubulin is blotted as a loading control. E. Western blot of endogenous FOXO3A and FOXO3B in LHCNM2 myoblasts from protein harvested in parallel with the RNA and gDNA. α-Tubulin is used as the loading control.

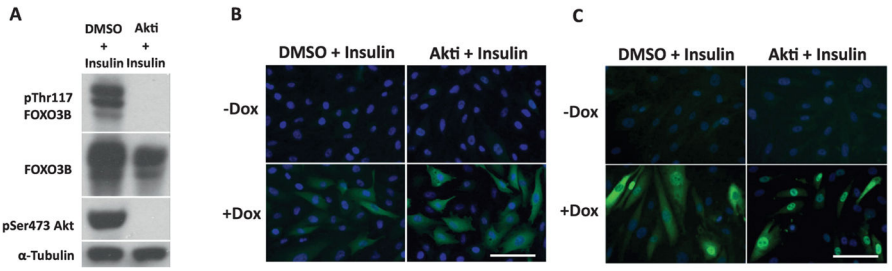

Fig. 4.

FOXO3B is phosphorylated by Akt on Thr117 but does not shuttle from the cytoplasm to the nucleus upon Akt inhibition. A. Western blot of LHCNM2 myoblasts overexpressing FOXO3B treated with DMSO (vehicle) and 200 nM insulin or 2 μM MK-2206 and 200 nM insulin for one hour. Phospho-Thr117 of FOXO3B was detected using an antibody raised against Thr24/32 of FOXO1/3 (Cell Signaling #9464). α-Tubulin is used as the loading control. B. Immunofluorescence of inducible FOXO3B overexpression in LHCNM2 myoblasts. +Dox cells were treated with 0.1 ug/ml Dox for 48 hours and then -/+ Dox cells were treated with DMSO and 200 nM insulin or 2 μM MK-2206 and 200 nM insulin for one hour. Blue is DAPI and green is staining with the FOXO3A antibody (Cell Signaling #2497) at a 1:1000 dilution. The white scale bar is 25 μm. C. A LHCNM2 myoblast line containing a Dox-inducible overexpression construct of wild-type FOXO3A. The cells were treated and stained as in Figure 4B. The white scale bar is 25 μm.